processes

MDPI

Article

Optimizing the Thickness of Multilayer Thermal Insulation on Different Pipelines for Minimizing Overall Cost-Associated Heat Loss

Mohammed R. A. Alrasheed

Department of Mechanical Engineering, King Saud University, Riyadh 11421, Saudi Arabia; mohalrasheed@ksu.edu.sa

Abstract: Optimizing the multilayer thermal insulation of pipelines transporting liquids and gases at higher than ambient temperatures is crucial for heat energy conservation and cost optimization. This study utilizes a multi-objective genetic algorithm to optimize the multilayer thermal insulation thickness around a pipe carrying fluid to minimize heat loss and associated costs. The model adopted mathematical associations between design variables and the overall installation cost of layers over a pipe from the available literature. The proposed model considered one or more insulation layers of rock wool and calcium silicate to oil pipelines containing steam, furfural, reduced crude or 300-distillate oil. All calculations considered fixed-charge rates as a fraction of 1 or 0.15. The results were compared with standard values and those predicted by other researchers in the literature. For the steam line, the standard insulation thickness was 50 mm, jumping to 327 mm for rock wool and 232 mm for calcium silicate. However, it decreased to 38 mm for double-layer calcium silicate and 138 mm for double-layer rock wool. For furfural, the insulation thickness was 40 mm, which rose to 159 mm for rock wool and 112 mm for calcium silicate. In general, for all four cases, the results show that using normal insulation thickness is inadequate and not economical. For example, for 300-distillate oil, the present practice puts the cost function at 54 USD/m, which drops to 20 USD/m for rock wool and 24 USD/m each for single-layer silicate and double-layer insulation. This amounts to almost 60% cost savings. Similar trends are observed for the other three cases. This model can provide up to 60% savings in cost and a 92% reduction in heat loss at optimum insulation thickness compared to other models.

Keywords: thermal insulation; multilayer insulation; multi-objective genetic algorithm; optimization; energy savings; life cycle cost analysis

check for updates

Citation: Alrasheed, M.R.A. Optimizing the Thickness of Multilayer Thermal Insulation on Different Pipelines for Minimizing Overall Cost-Associated Heat Loss. *Processes* **2024**, *12*, 318. https://doi.org/10.3390/pr12020318

Academic Editors: Li Xi and Federica Raganati

Received: 4 December 2023
Revised: 24 January 2024
Accepted: 27 January 2024
Published: 2 February 2024

Copyright: © 2024 by the author. Licensee MDPI, Basel, Switzerland. This article is an open access article distributed under the terms and conditions of the Creative Commons Attribution (CC BY) license (https://creativecommons.org/licenses/by/4.0/).

1. Introduction

Insulating materials have traditionally been employed to minimize thermal dissipation from surfaces operating at temperatures above the surrounding environment, such as pipes that convey liquids and gases. Multiple reports on the thermal insulation market have been published since 2022. Based on data from Precision Business Insights, the worldwide thermal insulation market had a value of USD 28.6 billion in 2022 and is projected to reach USD 35.6 billion by 2029, with a compound annual growth rate (CAGR) of 7.2% from 2024 to 2030 [1]. Precedence Research predicts that the building thermal insulation market will reach around USD 48.69 billion by 2032, up from its value of USD 32.74 billion in 2022, with a compound annual growth rate (CAGR) of 5.1%. IndustryARC, Telangana, India said the worldwide building thermal insulation market was valued at USD 29.75 billion in 2022 [2]. The Global Market Report for Building Thermal Insulation in 2023 forecasts that the global market for building thermal insulation will reach USD 44.69 billion by 2030, with a compound annual growth rate (CAGR) of 4.5% from 2023 to 2030 [3,4]. The reassessment of thermal insulation design has been motivated by recent concerns regarding energy conservation and the depletion of scarce energy resources. Nevertheless, the

most existing studies concentrate on the insulation of air-conditioned structures and cold-storage facilities, employing a flat plate or slab as the primary geometric arrangement, with particular emphasis on large-scale roofs and facades.

Although pipelines and cylindrical heat exchangers are commonly used in refineries, the chemical industry, and power plants, there is a lack of research on optimizing multilayer thermal insulation for cylindrical shapes [3,5]. In piping systems, it is customary to use a single layer of insulation to prevent heat transmission and maintain the insulated surface's temperature under a defined safety threshold.

Probert et al. [6] carried out preliminary research on using internal pipe lining to obtain the necessary level of thermal insulation to reduce energy loss rates. They developed equations that specifically addressed the most efficient dimensions for horizontal district-heating pipelines that transport hot water at a temperature of 95 °C.

A comprehensive literature survey on the critical insulation thickness for spherical and cylindrical geometries was provided by Aziz [7]. The author examined the most efficient arrangements for a circular pipe equipped with insulating elements an equilateral rectangular form, as well as polygonal and eccentric circular shapes. Additionally, the discussion encompassed several theoretical concepts. The two-dimensional conduction analysis revealed that for polygonal and rectangular geometries, the conduction remains consistent for the critical configuration, regardless of whether the outside surface boundary condition is convection or constant temperature. Kaynakli [8] conducted a comprehensive analysis of the most efficient thickness of thermal insulation on pipes or ducts with diverse geometries, such as circular forms, utilized in multiple sectors. The study compared the heat transfer equations, fundamental findings, optimization techniques, and economic analysis methodologies in different research investigations.

Khan et al. [9] examined the optimal thickness of thermal insulation materials for HVAC ducts with various shapes often found in buildings. The study demonstrated that incorporating an air gap and enhancing insulation at the compression site resulted in economic advantages, as determined through life cycle cost analysis and the consideration of environmental sustainability.

Powar and Dhamangaonkar [10] calculated the minimum insulation thickness required for ducts with a regular polygonal cross-section. A correction factor was used to multiply the critical thickness of circular cross-section insulation to obtain the polygonal cross-section value.

The viability of utilizing various insulation materials in pipelines has undergone thorough examination. Expanded polystyrene, rock wool, and extruded polystyrene are the materials that have been extensively researched [11]. Dasdemir et al. [12] optimized insulating layer thickness for HVAC applications using rock wool, expanded polystyrene, and extruded polystyrene materials with varying sizes of steel, plastic, and copper pipes. According to their findings, fuel oil and rock wool were the most cost-effective fuel and insulation material pairing. Ertürk [13] determined the optimal thickness values to be between 5 and 16 cm. Rosa and Bianco [14] studied the best conditions for steel pipes transporting warm water, considering technical, economic, and carbon emission limitations. They used three identical insulating materials for their analysis. The study revealed that the piping design, operating conditions, and heating system significantly influenced the appropriate insulation thickness. However, the impact of climatic conditions was minimal, particularly for fluid operating temperatures exceeding 45 °C.

Suresh et al. [15] utilized finite element-based methods to examine the heat dissipation at different process temperatures and for varied stainless-steel pipe diameters using three distinct insulating materials: expanded polystyrene, extruded polystyrene, and fiberglass. Theoretical calculations were employed to determine the most favorable insulation thickness based on factors, such as cost, heat loss of the system, and the temperature of the system's exterior surface. Using extruded polystyrene and fiberglass led to a favorable equilibrium of characteristics.

Salem et al. [16] examined the impact of varying insulation thickness using rock wool and polyurethane foam in their study. The decision to expand the use of polystyrene for the underground oil pipeline was based on a comprehensive evaluation of its life cycle costs and its susceptibility to economic factors and environmental pollutants. The study demonstrated that the ideal thickness for insulation ranged from 70.7 to 130.4 mm. Additionally, the corresponding yearly cost savings in energy varied between 403.69 and 419.29 USD/m, while the payback periods ranged from 0.331 to 0.887 years. Furthermore, the emissions reductions achieved at the most effective insulating layer were determined to be 93% for polyurethane foam, 90% for rock wool, and 93% for expanded polystyrene. Abujab and Abusafa [17] calculated the ideal insulation thickness for pipes in the Variable Refrigerant Flow system using the same three insulation materials. The researchers documented the most effective thicknesses of insulation materials for different pipe diameters. Rock wool had an ideal thickness range of 12.7–50.8 mm, extruded polystyrene, a range of 28–38 mm, and a flexible foam insulation range of 11–13 mm. These findings applied to pipe diameters ranging from 12.7 to 50.8 mm.

Ucar [18] conducted a thermo-economic analysis utilizing glass wool, expanded polystyrene, and expanded polystyrene materials to investigate the energy cost, exergy losses, and optimal insulation thicknesses of pipes in four Turkish towns with varying climatic conditions. The study directly correlated the ideal insulating thickness and degree days. Keçebaş et al. [19] studied rock wool's most effective insulation thickness for pipes used in district heating pipeline networks. The goal was to achieve energy savings over ten years. The study also examined the payback periods for five pipe sizes and four fuel types in Afyonkarahisar, Turkey. The findings indicated that the greatest energy conservation was achieved while employing a fuel–oil fuel type, with a nominal pipe size of 250 mm. Conversely, the smallest amount of energy savings was observed when utilizing a 50 mm pipe for geothermal energy.

Zhukov et al. [20] presented various techniques for computing polyethene foam insulation systems. The researchers assessed energy efficiency by measuring the environmental impact of insulating systems. The optimal thickness of polyethene foam was established to maintain a safe temperature to avoid moisture condensation on the insulating layer's surface.

Zhang et al. [21] examined the optimal conditions for using high-temperature-resistant glass wool, SiO_2 aerogel blanket, and aluminum silicate wool as insulation materials on steel pipes used for steam heating in urban districts. HTRGW and SAB demonstrated exceptional economic efficiency when operating under low-temperature circumstances. As the pipe diameter rose, the life cycle cost and economic thickness reduced dramatically, resulting in a corresponding rise in economic benefit.

Wang et al. [22] presented a novel gel thermal insulation material designed for steam pipelines. The material demonstrated excellent thermal insulation and waterproof capabilities. Krasnova [23] developed a novel type of multilayer thermal insulation consisting of a network of enclosed microvolumes (pores) filled with carbon dioxide and a high-density polyethene shell. This film can serve as a pre-made material for insulating pipelines.

There has been significant research on the mathematical modelling and simulation of thermal insulation in pipelines. Petal and Mehta [24] devised a computational algorithm to determine the most favorable thickness for cylindrical insulation. Their model considered the influence of wind speed and thermal radiation on the insulation thickness. However, their model failed to consider the optimal thickness, resulting in the lowest annual insulation cost.

Zhang et al. [25] simulated the temperature distribution in the insulation structure of the lower tank wall in a nuclear reactor. They then compared the simulation results with experimental data to validate their model's accuracy. The introduction of heat pipes in the initial concept resulted in a reduction in the structural load.

Sutheesh and Chollackal [26] thoroughly examined the multilayer insulation employed in cryogenics and space exploration initiatives. Dye et al. [27] effectively utilized Wrapped Multilayer Insulation to insulate pipelines and tubing that carry cryogenic fluids.

Afroozeh et al. [28] modified the grey wolf optimization method to address the economic–environmental dispatch problem in integrated combined heat and power systems. This optimization considered the impact of temperature decreases in heat pipes and the valve-point effect while dealing with heat solely and traditional thermal units. Their optimization findings demonstrated the superior performance of the suggested mutant grey wolf optimization method compared to existing metaheuristic algorithms.

Afra et al. [29] designed and built an experimental apparatus to study energy optimization in steam injection operations for improved oil recovery. An investigation was conducted to examine the impact of increasing the rate and temperature of steam injection and the application of nano-thermal insulators on the quantity of heat delivered to the reservoir. The application of nano-thermal insulators was found to be more technically and economically efficient than the other scenarios.

A study by Yang et al. [30] aimed to enhance the thermal insulation often employed in offshore oil production for flow assurance design. Integrating optimization methodology with machine learning approaches, a hybrid approach was introduced to identify the most cost-effective design. An evaluation was conducted on a subsea production system that utilized several insulation materials. The findings indicated that the suggested approach effectively determined material type and thickness variances across the subsea system, reducing cost. Kayfeci et al. [31] employed artificial neural networks (ANNs) to forecast the optimal insulation thickness and life cycle expenses for pipe insulation applications. The network produced the highest correlation coefficient while minimizing the error.

Xu et al. [32] demonstrated that integrating phase-change materials and traditional thermal insulation materials can significantly enhance the thermal insulation capabilities of oil pipelines.

Sahin and Kalyon [33] employed an analytical approach to examine the fluctuation in insulation thickness along a pipe carrying a high-temperature fluid to achieve a consistent outer surface temperature. The solution exhibited a nearly linear relationship, making it straightforward to execute.

The present study utilized a multi-objective genetic algorithm (MOGA) to optimize many performance characteristics of multilayer thermal insulation pipelines, including total cost, pressure drop, and insulation thickness. The work is founded on a notion articulated by Zaki and Al-Turki [34]. Their investigation employed the Hook and Jeeves model to determine the optimal thickness of insulation materials for the pipe network. The authors performed comprehensive economic research on various composite materials with varying characteristics and prices utilized in pipelines. The model was utilized for a system of four pipelines in an oil refinery. Their findings showed significant cost reductions when employing the methodology. The notable benefit of this solution's approach is its capacity to incorporate various constraints and safety requirements into selecting thermal insulation.

Zhang et al. [35] introduced an analytical technique to analyze multilayered pipes with temperature-dependent properties subjected to non-uniform pressure and thermal load. The study offered a thorough comprehension of the behavior of multilayered pipes in intricate circumstances, which might be valuable for designing and optimizing piping systems. The article introduced a technique for analyzing the performance of multilayered pipes with T-D characteristics subjected to non-uniform pressure and temperature load. Pipes exhibited temperature-dependent characteristics, implying their qualities vary in response to temperature. The pipes experienced non-uniform pressure and thermal load, which might impact their behavior and performance. The analytical approach outlined in the research can be utilized for many piping systems, including those employed in the oil and gas sector, power production, and other industrial operations.

Kim et al. [36] examined the application of multilayer vacuum-insulated pipes for transporting liquid hydrogen, a promising marine fuel that offers pollution reductions and high density. The article examined these pipes' thermal and structural properties, favored for conveying cryogenic liquids because of their safety, dependability, and cost-efficiency.

Zeng et al. [37] introduced a novel technique to quantify the vacuum level between layers in the multilayer insulating pipe used for liquified natural gas. This method entailed measuring the temperatures of the insulation pipe's outer and inner sides and utilizing these measurements to determine the interlayer vacuum level. The article elucidated the theoretical underpinnings of the approach and presented empirical evidence to substantiate its efficacy. The proposed approach has the potential to enhance the precision and effectiveness of measuring the interlayer vacuum level of the insulation pipe, which is crucial for guaranteeing the safety and dependability of liquified natural gas transportation.

Vakulenko et al. [38] investigated the phenomenon of thermal energy dissipation in insulated pipes and determined the critical threshold for insulation thickness. This article analyzed the correlation between heat resistance and the disparity in diameter between the outer and inner surfaces, along with its derivative. The study employed the formula for computing the mean heat transfer coefficient, incorporating the Grashof number. The essay stated that the thermal pipe insulation radius selection of technological equipment should be based on technical criteria.

Novelty/Contributions of this Work: This study employed a comparable methodology but utilized a distinct algorithm. The genetic algorithm was employed to optimize single- and two-layer thermal insulation around a pipe carrying a fluid above ambient temperature. This study aimed to minimize the overall associated costs and reductions in heat loss. It considered the single- or double-layer insulation of rock wool and calcium silicate around pipes carrying steam, furfural, reduced crude, or 300-distillate oil. The optimal thickness, overall associated costs, and reductions in heat loss were computed for all cases. The results are compared to the findings of Zaki [34]. The outcomes forecasted by this model exhibit a notable improvement in cost and heat loss reduction compared to the prognostications made by the model employed in Zaki (2000) [34].

Section 1 presents a comprehensive analysis of the existing literature to establish the background of this study and demonstrate its contribution to the current body of research. Section 2 pertains to the approach, while Section 3 encompasses the outcomes. Section 4 pertains to the analysis and interpretation of the findings, whereas Section 5 encompasses the final summary and overall conclusion.

2. Methodology

2.1. Cost Function

The function was derived considering a system of n pipes used to transport fluid (Figure 1) at different temperatures (T_{f1}, T_{f2}, T_{f3},..., T_{fj}...T_{fn}) from pipelines, where the fluid temperature is greater than the ambient temperature T_a. Lengths (l_1, l_2, l_3,..., l_j...l_n) and outer radii (a_1, a_2, a_3,..., a_j...a_n) of pipes (n) are given. The thickness of the pipes is neglected in calculations. The piping system is insulated with m_j insulating layers to reduce heat loss. The outer and inner radii of the i^{th} insulation layer in the j^{th} pipe are given as $r_{j,i+1}$ and $r_{j,i}$. The outer radius of the outermost insulation layer is b_j.

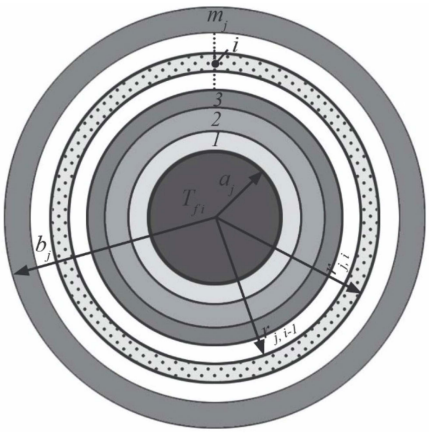

Figure 1. Top view of i^{th} pipe carrying fluid at a temperature T_{fi} protected with m_j insulating layers.

2.2. Initial Investment Cost of Insulation

The total initial investment cost of applying m_j insulating layers around n pipelines is given as Equation (1), where $c_{j,i}$ is the insulation cost per unit length of the i^{th} layer of the j^{th} pipe [34].

$$C = \sum_{j=1}^{n} \sum_{i=1}^{m_j} c_{j,i} \pi \left[r_{j,i+1}^2 - r_{j,i}^2 \right] l_j \quad (1)$$

2.3. Cost of Heat Loss

Heat transfer rate per unit length in the j^{th} pipe ($j \in [1, 2, 3, \ldots n]$) at steady state is given as Equation (2) [34].

$$q_j = \frac{T_{fj} - T_a}{R_j} \quad (2)$$

where T_{fj} is the temperature inside the j^{th} the pipe carrying the fluid, T_a is the ambient temperature, and R_j denotes the overall thermal resistance of the composite insulating material of the j^{th} pipe with m_j insulating layers. If b_j is the outermost radius of the insulation composite, R_j is given by Equation (3), where k_{ji} is the thermal conductivity of the i^{th} layer of the j^{th} pipe, and h_a is the heat transfer coefficient [34].

$$R_j = \frac{1}{2\pi a_j h_{fj}} + \sum_{i=1}^{m_j} \frac{\ln\left(\frac{r_{i+1}}{r_i}\right)}{2\pi k_{ji}} + \frac{1}{2\pi b_j h_a} \quad (3)$$

The total energy loss from n pipes annually is given by Equation (4) [34].

$$Q = \int_0^{\varphi_j} q_j l_j d\varphi \quad (4)$$

where φ_j is the annual operation period of each pipeline. If the system works around the clock, $\varphi_j = 8760$ h. The cost incurred due to the loss of heat Q is given by Equation (5) [34].

$$C_e = c_e Q \quad (5)$$

where c_e is the cost of heat per kilowatt hour.

2.4. Overall Cost

The total cost of applying insulating layers and fluid flow is calculated using Equations (1) and (5), as given by Equation (6), where f denotes the fixed-charges rates, including interest and depreciation [34].

$$Z = fC + C_e \quad (6)$$

Z is the fitness function with m_j unknown variables of insulation thickness ($\delta_1, \delta_2, \ldots \delta_i, \ldots \delta_{m_j}$) to be optimized. The multi-objective genetic algorithm optimization technique (MOGA) is used to optimize Equation (6). A schematic diagram of MOGA is given in Figure 2. A new population of sets of succeeding generations was selected through selection, mutation, and crossover of the preceding generation. Optimal structural and insulation layer thickness values were computed. A double-vector population type with a size of 30 was used. The crossover was 0.8, and the mutation function was constraint-dependent. The intermediate crossover function had a ratio of 1. Migration was implemented forward with a fraction of 0.2 and an interval of 20. The Pareto front population function was 0.35. Termination criteria were selected, with the maximum number of generations and the minimum fitness function value selected as 400 and 10^{-4}, respectively.

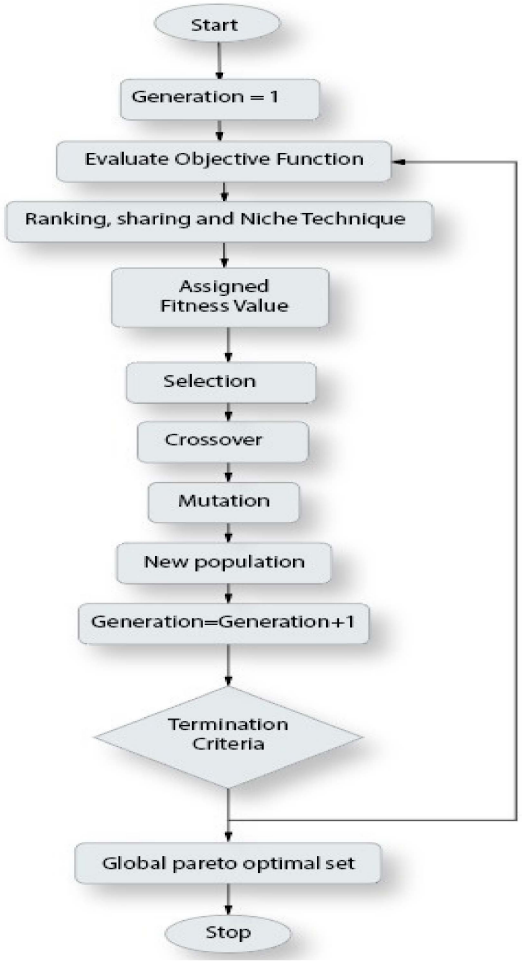

Figure 2. Schematic flow diagram of multi-objective genetic algorithm.

2.5. System Constraints

The composite cylindrical geometry imposes certain system constraints. The inner radius of an insulating layer must be greater than the outer radius of the previous sub-layer. Moreover, the thickness of the insulation layer δ_i should be between limits δ_{min} and δ_{max}, specified by the available thicknesses of different types of insulation. Equations (7) and (8) mathematically express these constraints [34]. Note that δ_{min} is assumed to be 38 mm and δ_{max} of a layer at the j^{th} pipe to be five-times the radius of the pipe.

$$r_{j,i} > r_{j,i-1} \tag{7}$$

$$\delta_{max} \geq r_{j,i} - r_{j,i-1} \geq \delta_{min} \tag{8}$$

In addition, the temperature of the outermost layer should not be more than 60 °C to avoid any fire hazard. Mathematically, this can be expressed as Equation (9), an essential physical condition to satisfy [34]. Here, R_{0j} is the heat transfer resistance of the outermost insulation layer with radius b_j.

$$T_{fj} - \left(T_{fj} - T_a\right)\frac{R_{0j}}{R_j} \leq 60 \tag{9}$$

Accordingly, the fitness function is given as Equation (10).

$$\begin{gathered} \text{Minimize } Z(\delta_1,\ \delta_2, \ldots \delta_i, \ldots\ \delta_{m_j}) = fC + C_e \\ \text{Subject to : } r_{j,i} > r_{j,i-1} \text{ and } \delta_{max} \geq r_{j,i} - r_{j,i-1} \geq \delta_{min} \end{gathered} \tag{10}$$

The multilayer thermal insulation applicable in the oil industry was optimized using Equation (10). Four pipeline systems were considered, and the parameters are given in Table 1. Here, $T_a = 50$ °C, $h_a = 10$ W/m^{2}K, and $c_e = 0.02$ \$/kWh. Z is optimized, keeping f equal to 0.15 and 1, considering the four pipeline systems. The results of using different insulation layers are compared with the present thermal insulation of rock wool, whose thickness is given in Table 1.

Table 1. Pipeline identification, specifications, fluid flow parameters, and insulation thickness used in the oil industry [34].

Serial No.	Pipeline Identification	Nominal Size of Pipe (mm)	Outer Radius (mm)	Actual Radius (mm)	T_f (°C)	h_f (W/m^{2}K)	Present Rock Wool Insulation Thickness (mm)
1	steam line	254.0	142.8	149.2	400.0	55.0	50.0
2	furfural	203.2	105.0	109.0	170.0	1500.0	40.0
3	reduced crude	152.4	78.5	84.0	270.0	1200.0	40.0
4	300-distillate oil	101.6	54.0	57.0	290.0	899.2	25.0

The optimization used two types of insulation material: rock wool and calcium silicate. The initial investment cost per unit length of insulating with rock wool is 146.7 USD/m^3 with a thermal conductivity of 0.06 W/m·K, and with calcium silicate amounting to 336 USD/m^3 with a thermal conductivity of 0.051 W/m·K. The thermal conductivity of the insulating materials varies linearly within a temperature range of 50–400 °C. The thermal conductivities of rock wool and calcium silicate at 50 °C are 0.038 and 0.051 W/m·K, respectively. The corresponding figures at 400 °C are 0.12 and 0.11 W/m·K, respectively. The optimization of the cost function (Equation (10)) is computed for four situational responses:

(a) Present insulation;
(b) Optimum single-layer rock wool;
(c) Optimum single-layer calcium silicate;
(d) Optimum double layer, with calcium silicate followed by rock wool insulation.

2.6. Mathematical Formulation for Single-Layer Insulation (m_j = 1)

Initial investment for one layer of insulation can be represented by Equation (11), where c_j is the initial insulation cost per unit length, and $x_{1,1}$, $x_{2,1}$, $x_{3,1}$, and $x_{4,1}$ are unknown outer-insulation-layer radii (b_1, b_2, b_3, and b_4) of pipelines carrying (a) steam line, (b) furfural, (c) reduced crude, and (d) 300-distillate oil [34].

$$C(x_{1,1},\ x_{2,1},\ x_{3,1},\ x_{4,1}) = \sum_{j=1}^{n=4} c_j \pi \left[x_{j,1}^2 - a_j^2 \right] l_j \tag{11}$$

Heat transfer rate per unit length in the j^{th} pipe ($j \in [1,4]$) can be expressed by Equation (12), where k_j is the thermal conductivity of the j^{th} insulation material layer [34].

$$q_j(x_{j,1}) = \frac{T_{fj} - T_a}{\frac{1}{2\pi a_j h_{fj}} + \frac{ln\left(\frac{x_{j,1}}{a_j}\right)}{2\pi k_j} + \frac{1}{2\pi x_{j,1} h_a}} \tag{12}$$

Linear inequality constraints for Equations (7) and (8) are represented mathematically in Equation (13).

$$\begin{bmatrix} -1 & 0 & 0 & 0 \\ 0 & -1 & 0 & 0 \\ 0 & 0 & -1 & 0 \\ 0 & 0 & 0 & -1 \\ 1 & 0 & 0 & 0 \\ 0 & 1 & 0 & 0 \\ 0 & 0 & 1 & 0 \\ 0 & 0 & 0 & 1 \\ -1 & 0 & 0 & 0 \\ 0 & -1 & 0 & 0 \\ 0 & 0 & -1 & 0 \\ 0 & 0 & 0 & -1 \end{bmatrix} \begin{bmatrix} x_{1,1} \\ x_{2,1} \\ x_{3,1} \\ x_{4,1} \end{bmatrix} \leq 10^{-3} \begin{bmatrix} -492 \\ -109 \\ -84 \\ -57 \\ 895.2 \\ 654 \\ 504 \\ 342 \\ -298.4 \\ -218 \\ -168 \\ -114 \end{bmatrix} \tag{13}$$

2.7. Mathematical Formulation for Double-Layer Insulation (m_j = 2)

The initial investment of a double layer of insulation can be written as Equation (14), where c_j is the initial insulation cost per unit length, and $x_{1,1}$, $x_{2,1}$, $x_{3,1}$, and $x_{4,1}$ are the unknown outer radii of the first insulation layer (i.e., calcium silicate) of pipelines (a), (b), (c), and (d), respectively [34].

$$\begin{aligned} &C(x_{1,1},\ x_{2,1},\ x_{3,1},\ x_{4,1},\ x_{1,2},\ x_{2,2},\ x_{3,2},\ x_{4,2}) \\ &= \sum_{j=1}^{n=4} c_{j,1}\pi\left[x_{j,1}^2 - a_j^2\right]l_j \\ &+ \sum_{j=1}^{n=4} c_{j,2}\pi[x_{j,2}^2 - x_{j,1}^2]l_j \end{aligned} \tag{14}$$

ublend (9), are given as Equation (14) f insulation layer. inwool ulation layers.

Similarly, $x_{1,2}$, $x_{2,2}$, $x_{3,2}$, and $x_{4,2}$ are unknown outer radii of the second insulation layer (i.e., rock wool).

Heat transfer rate per unit length in the j^{th} pipe ($j \in [1,4]$) can be written as Equation (15), where $k_{j,1}$ and $k_{j,2}$ are the thermal conductivities of calcium silicate and rock wool insulation layers, respectively. Similarly, $x_{j,1}$ and $x_{j,2}$ are the outer radii [34].

$$q_j(x_{j,1},\ x_{j,2}) = \frac{T_{fj} - T_a}{\frac{1}{2\pi a_j h_{fj}} + \frac{ln\left(\frac{x_{j,1}}{a_j}\right)}{2\pi k_{j,1}} + \frac{ln\left(\frac{x_{j,2}}{x_{j,1}}\right)}{2\pi k_{j,1}} + \frac{1}{2\pi x_{j,2} h_a}} \tag{15}$$

Linear inequality constraints for Equations (8) and (9) are represented mathematically by Equation (16).

$$\begin{bmatrix} -1 & 0 & 0 & 0 & 0 & 0 & 0 & 0 \\ 1 & -1 & 0 & 0 & 0 & 0 & 0 & 0 \\ -1 & 0 & 0 & 0 & 0 & 0 & 0 & 0 \\ 1 & 0 & 0 & 0 & 0 & 0 & 0 & 0 \\ 1 & -1 & 0 & 0 & 0 & 0 & 0 & 0 \\ -6 & 1 & 0 & 0 & 0 & 0 & 0 & 0 \\ 0 & 0 & -1 & 0 & 0 & 0 & 0 & 0 \\ 0 & 0 & 1 & -1 & 0 & 0 & 0 & 0 \\ 0 & 0 & -1 & 0 & 0 & 0 & 0 & 0 \\ 0 & 0 & 1 & 0 & 0 & 0 & 0 & 0 \\ 0 & 0 & 1 & -1 & 0 & 0 & 0 & 0 \\ 0 & 0 & -6 & 1 & 0 & 0 & 0 & 0 \\ 0 & 0 & 0 & 0 & -1 & 0 & 0 & 0 \\ 0 & 0 & 0 & 0 & 1 & -1 & 0 & 0 \\ 0 & 0 & 0 & 0 & -1 & 0 & 0 & 0 \\ 0 & 0 & 0 & 0 & 1 & 0 & 0 & 0 \\ 0 & 0 & 0 & 0 & 1 & -1 & 0 & 0 \\ 0 & 0 & 0 & 0 & -6 & 1 & 0 & 0 \\ 0 & 0 & 0 & 0 & 0 & 0 & -1 & 0 \\ 0 & 0 & 0 & 0 & 0 & 0 & 1 & -1 \\ 0 & 0 & 0 & 0 & 0 & 0 & -1 & 0 \\ 0 & 0 & 0 & 0 & 0 & 0 & 1 & 0 \\ 0 & 0 & 0 & 0 & 0 & 0 & 1 & -1 \\ 0 & 0 & 0 & 0 & 0 & 0 & -6 & 1 \end{bmatrix} \begin{bmatrix} x_{1,1} \\ x_{1,2} \\ x_{2,1} \\ x_{2,2} \\ x_{3,1} \\ x_{3,2} \\ x_{4,1} \\ x_{4,2} \end{bmatrix} \leq 10^{-3} \begin{bmatrix} -149.2 \\ 0 \\ -187.2 \\ 895.2 \\ -38 \\ 0 \\ -109 \\ 0 \\ 147 \\ 654 \\ -38 \\ 0 \\ -84 \\ 0 \\ 122 \\ 504 \\ -38 \\ 0 \\ -57 \\ 0 \\ -95 \\ 342 \\ -38 \\ 0 \end{bmatrix} \tag{16}$$

3. Results

The optimization technique converged after 200 iterations. A comparative analysis of the costs associated with single-layer rock wool (RW), single-layer calcium silicate (CS), and double-layer (RS + CS) insulation with the normal practice (P) of using the thickness of RW (P) at $f = 0.15$ is given in Figure 3 and Table 2. In general, for all four cases, the results show that using normal insulation thickness is inadequate and not economical.

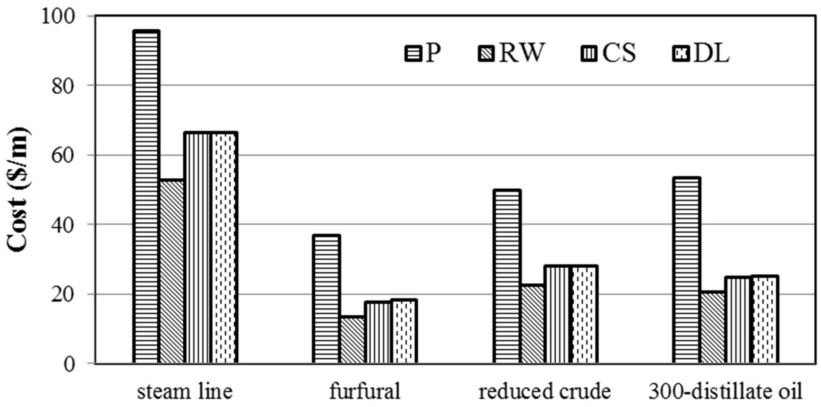

Figure 3. Comparative analysis of cost associated (at $f = 0.15$) with single-layer rock wool (RW), single-layer calcium silicate (CS) and double insulation (DL) of CS and RW with the normal insulation thickness RW (P).

Table 2. Values of overall cost associated with insulation, reduced heat loss, and optimal insulation thickness using single-layer rock wool (RW), single-layer calcium silicate (CS), double-layer RW + CS compared to the standard values (P) [34] at $f = 0.15$.

	Steam Line	Furfural	Reduced Crude	300-Distillate Oil
		Cost (USD/m)		
P	96	37	50	54
RW	53	14	22	20
CS	66	18	28	25
DL	67	18	28	25
		Q (W/m)		
P	405	155	211	228
RW	110	27	48	45
CS	134	34	57	53
DL	90	22	39	19
		δ (mm)		
P	50	40	40	25
RW	327	159	216	208
CS	232	112	154	149
DLCS	38	39	38	39
DLRW	108	38	64	58

For example, for 300-distillate oil, the present practice puts the cost function at 54 USD/m, which drops to 20 USD/m for rock wool and 24 USD/m each for single-layer silicate and double-layer insulation. This amounts to almost 60% in cost savings. Similar trends are observed for the other three cases.

For the steam line, using normal insulation thickness, RW (P) puts the cost function at 96 USD/m, which drops to 53 USD/m for rock wool (45% reduction) and 66 USD/m each for single-layer silicate and double-layer insulation. For furfural, the cost function is 37 USD/m, which drops to 14 USD/m for rock wool (62% reduction) and 18 USD/m each for single- and double-layer silicate.

Similarly, the comparative responses of heat loss and optimal insulation thickness (at $f = 0.15$) after insulation within the four cases are shown in Figures 4 and 5, respectively. The corresponding values are given in Table 2. Although minimum cost is associated with the RW layer, as shown in Figure 3, the RW layer at the steam line pipeline generates the least heat. However, optimal thickness is higher with single-layer CS than with single-layer RW and CS + RW. Maximum heat is lost in the steam line pipe using RW (P). However, the heat loss is reduced significantly in all three types of insulation considered in this model. The heat losses within a particular type of pipeline do not show much variation for the three types of insulation, as shown in Figure 4.

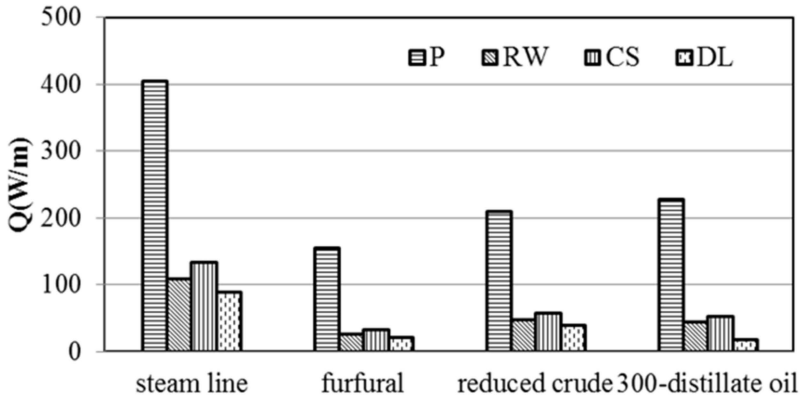

Figure 4. Comparative analysis of heat loss (at $f = 0.15$) after insulation with (i) single-layer RW, (ii) single-layer CS and (iii) CS and RW layers with the normal insulation thickness RW (P).

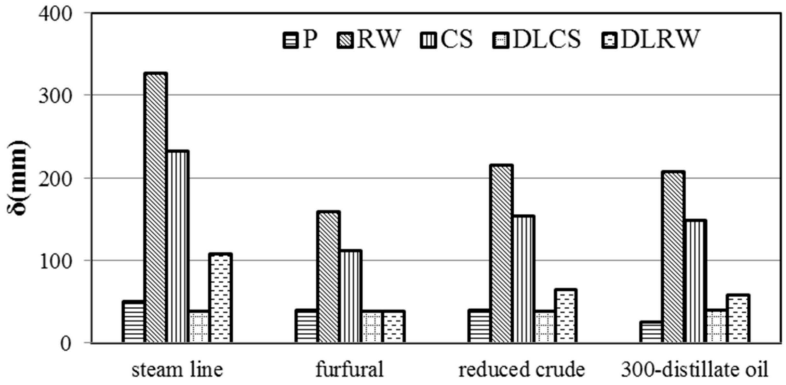

Figure 5. Comparative analysis of optimum insulation thickness δ (at $f = 0.15$) after insulation with (i) single-layer RW, (ii) single-layer CS and (iii) double-layer CS (DLCS) and double-layer RW (DLRW) layers with the normal insulation thickness RW (P).

The heat loss using RW (P) for the steam line is 405 W/m, which is reduced to 90 W/m for double-layer insulation using the RW (P) model. This is an almost 78% reduction in heat loss. On the other hand, for 300-distillate oil, the heat loss using the RW (P) model is 228 W/m, which is reduced to 19 W/m in this model. This is an almost 92% reduction in heat loss. The percentage reductions in heat loss for furfural and reduced crude predicted by this model are 86% and 82%, respectively.

The optimum insulation thickness data (Figure 5) show a similar trend for the four insulations, as shown in Figure 4. The maximum insulation thickness is predicted for rock

wool, followed by calcium silicate, double-layer rock wool and double-layer calcium silicate. Compared to using RW (P), the rock wool and single-layer calcium silicate thicknesses are much higher. Still, the double-layer insulations are at a thickness comparable to the present practice. We take the steam line and furfural as the two representative cases. For the steam line, the insulation thickness is 50 mm, which jumps to 327 mm for rock wool and 232 mm for calcium silicate. However, it comes down to 38 mm for double-layer calcium silicate and 138 mm for double-layer rock wool. For furfural, the present insulation thickness is 40 mm, which rises to 159 mm for rock wool and 112 mm for calcium silicate. It is similar to the present value for both double-layer insulations.

A comparative analysis of the costs associated with single-layer RW, single-layer CS, and double-layer RS + CS insulation with the present practice (P) of using the standard thickness of RW (P) at $f = 1$ is given in Figure 6 and Table 3. The results are not significantly different from those for f = 0.15 (Figure 3).

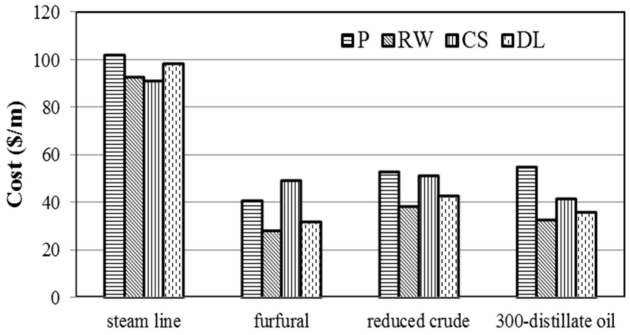

Figure 6. Comparative analysis of costs associated (at $f = 1$) with single-layer rock wool (RW), single-layer calcium silicate (CS) and double insulation of CS and RW with the present (P) practice using RW (P) insulation.

Table 3. Values of overall costs associated with insulation, reduced heat loss and optimal insulation thickness using single-layer rock wool (RW), single-layer calcium silicate (CS), double-layer RW + CS compared to the standard values (P) [34] at $f = 1$ [2].

	Steam Line	**Furfural**	**Reduced Crude**	**300-Distillate Oil**
		Cost (USD/m)		
P	102	41	53	55
RW	93	28	38	33
CS	91	34	51	42
DL	98	32	43	36
		Reduced heat loss (W/m)		
P	405	159	211	228
RW	177	35	75	67
CS	182	41	83	83
DL	153	29	74	66
		Insulation thickness (mm)		
P	50	40	40	25
RW	148	108	98	96
CS	148	108	83	66
DLCS	38	37	38	38
DLRW	106	41	62	60

For the steam line, no significant reduction in costs is predicted for the three insulations. However, the other three pipelines show considerable reductions in costs. For example, for 300-distillate oil, the cost of using RW (P) is 55 USD/m, which is reduced to 33, 42, and 46 USD/m for rock wool, calcium silicate, and double-layer insulations, respectively.

Similarly, the comparative response of heat loss and optimal insulation thickness (at $f = 1$) after insulation for the four cases is shown in Figures 7 and 8, respectively. The corresponding values are given in Table 3. The results are close to f = 0.15 (Figures 4 and 5) amongst the different insulations.

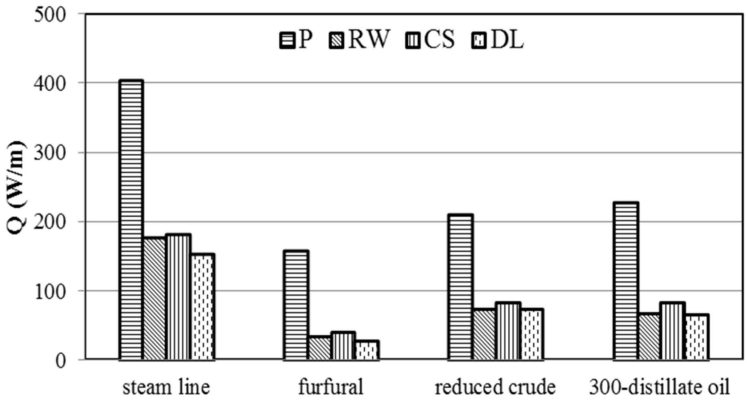

Figure 7. Comparative analysis of heat loss (at $f = 1$) after insulation with (i) single-layer RW, (ii) single-layer CS and (iii) CS and double-layer CS and RW layers with the present (P) practice of using RW (P) insulation.

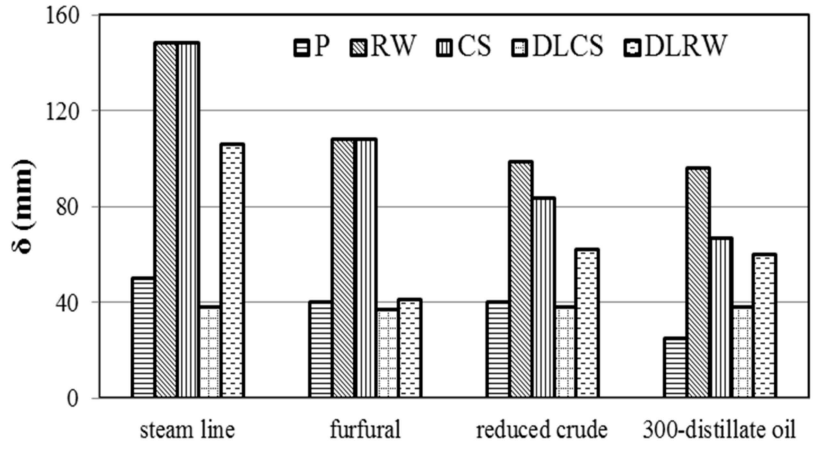

Figure 8. Comparative analysis of optimum insulation thickness δ (at $f = 1$) after insulation with (i) single-layer RW, (ii) single-layer CS and (iii) double-layer CS (DLCS) and double-layer RW (DLRW) layers with the present (P) practice of using RW (P) insulation.

As in the previous case, we discuss steam line and 300-distillate oil as the representative cases. The heat loss using RW (P) for the steam line is 405 W/m, which is reduced to 153 W/m for double-layer insulation in the present model. This is an almost 62% reduction in heat loss. On the other hand, for 300-distillate oil, the heat loss using RW (P) is 228 W/m, which is reduced to 66 W/m in this model. This is an almost 71% reduction in heat loss. The percentage reductions in heat loss for furfural and reduced crude predicted by this model are 78% and 65%, respectively. This model predicts much higher heat loss values for f = 0.15 than f = 1.0.

The optimum insulation thickness follows a similar pattern for f = 0.15 for individual pipeline systems. The maximum thickness is for rock wool, followed by calcium silicate, double-layer rock wool, and double-layer calcium silicate.

Percentage reductions in heat produced for all four cases are calculated to put the results in perspective. Figures 9 and 10 show the percentage reduction in heat loss using optimal thickness at $f = 0.15$ and 1, respectively. The maximum reduction in heat using any of the four pipelines is attained using DL CS + RW insulation layers at $f = 0.15$. Distillate oil pipelines reduce the most heat compared to the other pipelines. At $f = 1$, CS + RW insulation is better but not significantly different than other insulation cases.

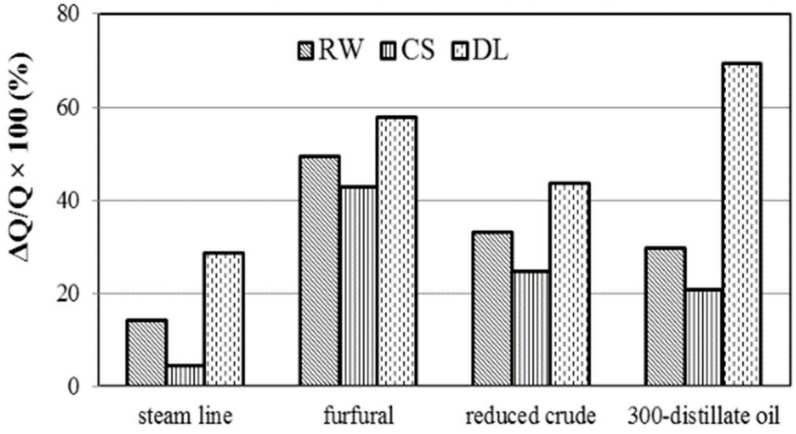

Figure 9. Percentage heat reduced (at $f = 0.15$) due to insulation layers compared to the present (P) practice of using RW (P) insulation.

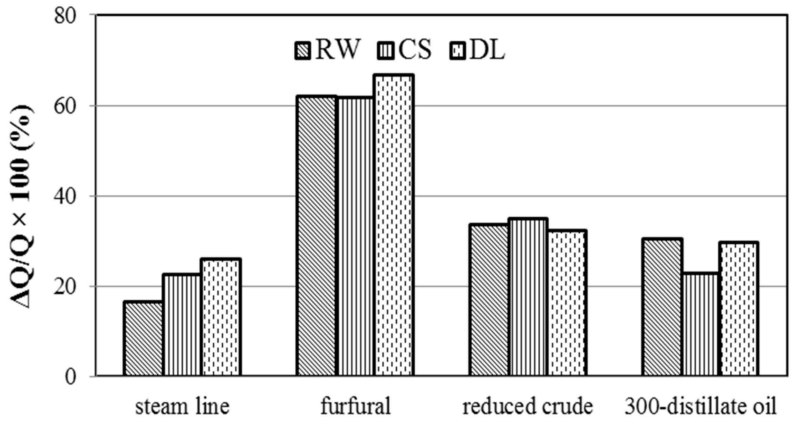

Figure 10. Percentage heat reduced (at $f = 1$) due to insulation layers compared to the present (P) practice of using RW (P) insulation.

4. Discussion

The worldwide emphasis on energy conservation has elicited an active response from academics and researchers, and they are coming up with new theories and models to mitigate energy losses in different applications. One such application is the transportation of fluids with higher than ambient temperatures in pipelines for various industries using multilayer insulation. This paper employed the MOGA optimization method for solving a mathematical thermal insulation model. This method is based on a multi-objective genetic algorithm. It aimed to optimize multilayer thermal insulation thickness based on pipeline performance parameters, such as cost, heat loss, and insulation thickness.

The model is applied to the real-world application of four pipelines used in the oil industry for transporting steam, furfural, reduced crude, and 300-distillate oil in pipes insulated by rock wool, calcium silicate, and double layers of these two materials. The results showed that using insulation thickness RW (P) is inadequate for all four cases and far from economical. The cost savings predicted by this model are up to 60%, and the heat loss is reduced by up to 92% compared to RW (P). This study investigated the heat loss,

the thickness of multilayer insulation materials, and insulation costs for different fluid line pipes. The predicted insulation cost was compared with a study by Zaki and Turki, who applied the Hook and Jeeves model (HJ). A comparison of the most important parameter, the cost function, using the present algorithm and Hook and Jeeves' optimization algorithm for f = 0.15 is shown in Table 4. GA predicted a lower cost than the HJ algorithm, stating that GA is a promising technique for optimizing thermal insulation problems.

Table 4. Cost functions (USD/m) predicted by Hook and Jeeves (HJ) and multi-objective genetic algorithm MOGA for four insulation systems.

	Present Practice		**Single Layer Rock Wool**		**Single Layer CS**		**Double Layer CS + RW**	
Pipeline system	HJ	MOGA	HJ	MOGA	HJ	MOGA	HJ	MOGA
Superheated	96	96	53	42	66	48	54	42
Furfural	37	37	18	14	21	18	20	18
Reduced crude	50	50	22	22	28	25	25	14
300-distillate	53	53	20	20	25	21	25	19

5. Conclusions

The genetic algorithm, a population-based optimization technique, is promising for optimizing single- and multilayer thermal insulation over different pipelines carrying fluid above ambient temperature. This technique provided better results than the Hook and Jeeves algorithm, which is expected to reduce cost savings by up to 66% and heat loss by 92%. This study tested the considered numerical model with four pipelines used in the oil industry for transporting steam, furfural, reduced crude, and 300-distillate oil. The insulation materials studied were rock wool, calcium silicate, and double layers of these two materials. The results showed that using insulation thickness RW (P) is inadequate for all four cases and far from economical. The concluding findings from the study are as follows:

The heat loss was reduced by 78% compared to the standard value of 405 W/m at f = 0.15 using double-layer insulation of RW and CS in the steam line pipeline. Similarly, furfural pipelines reduced heat loss by up to 86%. Double-layer insulation reduced heat loss by up to 81% using a reduced crude pipeline. Double-layer insulation of CS and RW significantly reduced heat loss by 92% compared to the present standard value of 405 W/m. The corresponding values of reduction in heat loss by single-layer RW were not significantly different for all four pipelines than double-layer CS + RW. Single-layer CS reduces the minimum and maximum heat loss of 67% and 78% in all considered pipelines.

Considering f = 0.15, the predicted overall associated cost reduction by the genetic algorithm was up to 63% compared to the predicted by the Hook and Jeeves algorithm using a single-layer RW insulation layer for a pipeline carrying furfural or 300-distillate oil. The minimum cost reduction was 45% when using single-layer RW in the carrying pipeline. At f = 1, the minimum and maximum cost savings compared to standard values were 9% and 40% for steam and 300-distillate oil-carrying pipelines, respectively. At f = 0.15, the overall associated cost reductions in single-layer CS and double-layer RW + CS did not differ considerably. For example, both kinds of insulation reduced costs in the steam pipeline by up to 30%. It was 44% for both insulations in crude oil-carrying pipelines.

This study reported the optimum insulation thicknesses for all these cost savings and heat losses. These values significantly minimize heat loss and overall associated costs compared to standard present values in the literature. Moreover, it was seen that GA predicted much better results compared to those previously reported by other researchers. Hence, the reported model can be used for real-world applications across various industries using pipelines for transporting liquids and gases at higher than ambient temperatures.

Funding: The author thanks the Deputyship for Research and Innovation, "Ministry of Education" in Saudi Arabia, for funding this research (IFKSUOR3-046-5).

Data Availability Statement: Data are contained within the article.

Conflicts of Interest: The author has no conflicts of interest to declare. The author has no relevant financial or non-financial interests to disclose.

Nomenclature

$a_1, a_2, a_3, \ldots, a_j \ldots a_n$	the outer radius of different pipelines (mm)
b_j	the outer radius of the outermost insulation layer (mm)
$c_{j,i}$	insulation cost per unit length of the i^{th} layer of the j^{th} pipe (USD/mm)
C_e	the cost incurred due to the loss of Q
c_e	cost of heat per kilowatt hour ($/kWh)
C	total initial investment cost of applying m_j Insulating layers around n pipelines (USD/m)
c_j	initial insulation cost per unit length (USD/mm)
f	fixed charges rates, including interest and depreciation
h_a	the heat transfer coefficient (W/m^{2}K)
k_{ji}	thermal conductivity of the i^{th} layer of the j^{th} pipe (W/mK)
$l_1, l_2, l_3, \ldots, l_j \ldots l_n$	length of different pipelines (mm)
m_j	number of insulation layers in j^{th} pipeline in the system
n	number of pipelines in the system
Q	total energy loss from n pipes annually (J)
$r_{j,i+1}$	the outer radius of the i^{th} insulation layer in the j^{th} pipe (mm)
$r_{j,i}$	the inner radius of the i^{th} insulation layer in the j^{th} pipe (mm)
R_j	the overall thermal resistance of the composite insulating material of the j^{th} pipe with m_j insulating layers (m^{2}K/W)
R_{0j}	heat transfer resistance of the outermost insulation layer
$T_{f1}, T_{f2}, T_{f3}, \ldots, T_{fj} \ldots T_{fn}$	the temperature of the fluid in different pipelines (K)
T_a	ambient temperature (K)
T_{fj}	temperature inside the j^{th} the pipe carrying the fluid (K)
T_a	ambient temperature (K)
$x_{1,1}, x_{2,1}, x_{3,1}$, and $x_{4,1}$	unknown outer insulation layer radii (b_1, b_2, b_3, and b_4) of pipelines carrying (a) steam line, (b) furfural, (c) reduced crude, and (d) 300-distillate oil (mm)
Z	fitness function with m_j unknown variables of insulation thickness ($\delta_1, \delta_2, \ldots \delta_i, \ldots \delta_{m_j}$) to be optimized
δ_{min} and δ_{max}	minimum and maximum range of an insulating material (mm)
φ_j	operation period of each pipeline annually (hours)

References

1. Available online: https://www.precisionbusinessinsights.com/market-reports/thermal-insulation-market (accessed on 20 January 2024).
2. Available online: https://www.precedenceresearch.com/building-thermal-insulation-market (accessed on 20 January 2024).
3. Wu, K.; Wang, R.; Ye, Z.; Tao, Y.; Wu, H.; Sun, W.; Cheng, J.; Kuang, Y.; Jiang, F.; Chen, S. The Optimization of Thermal Insulation-Related Properties of Polysaccharide-Based Aerogel by the Multilayer Combination Method. *J. Porous Mater.* **2023**, *30*, 1449–1458. [CrossRef]
4. Furion Analytics Research & Consulting LLP. *Building Thermal Insulation Market Overview*; Furion Analytics Research & Consulting LLP: Telangana, India, 2024.
5. Sun, W.; Liu, Y.; An, Q.; Huang, S.; Li, F. Stress Characteristics and Structural Optimization of Spacecraft Multilayer Insulation Components. *Aerospace* **2023**, *10*, 577. [CrossRef]
6. Probert, S.D.; Chu, C.Y.; Yeung, C.M. A Possible Alternative Approach to the Thermal Insulation of Pipelines. *Appl. Energy* **1982**, *11*, 15–34. [CrossRef]
7. Aziz, A. The Critical Thickness of Insulation. *Heat Transf. Eng.* **1997**, *18*, 61–91. [CrossRef]
8. Kaynakli, O. Economic Thermal Insulation Thickness for Pipes and Ducts: A Review Study. *Renew. Sustain. Energy Rev.* **2014**, *30*, 184–194. [CrossRef]
9. Khan, M.H.; Abro, M.A.; Soomro, J.; Aftab, Y.; Kumar, D. Optimum Insulation Thickness for HVAC Duct: An Energy Conservation Measure. *Eng. Sci. Technol. Int. Res. J.* **2018**, *2*, 53–62.

10. Powar, S.B.; Dhamangaonkar, P.R. Estimation of Critical Thickness of Insulation for Regular Polygon Cross-Section Ducts/Conductors. *Mater. Today Proc.* **2023**, *72*, 1712–1719. [CrossRef]
11. Superti, V.; Forman, T.V.; Houmani, C. Recycling Thermal Insulation Materials: A Case Study on More Circular Management of Expanded Polystyrene and Stonewool in Switzerland and Research Agenda. *Resources* **2021**, *10*, 104. [CrossRef]
12. Daşdemir, A.; Ural, T.; Ertürk, M.; Keçebaş, A. Optimal Economic Thickness of Pipe Insulation Considering Different Pipe Materials for HVAC Pipe Applications. *Appl. Therm. Eng.* **2017**, *121*, 242–254. [CrossRef]
13. Ertürk, M. Optimum Insulation Thicknesses of Pipes with Respect to Different Insulation Materials, Fuels and Climate Zones in Turkey. *Energy* **2016**, *113*, 991–1003. [CrossRef]
14. De Rosa, M.; Bianco, V. Optimal Insulation Layer for Heated Water Pipes under Technical, Economic and Carbon Emission Constraints. *Energy* **2023**, *270*, 126961. [CrossRef]
15. Suresh, S.; Sundar, M.; Lokavarapu, B.R. Optimum Insulation Thickness in Process Pipelines. *Mater. Today Proc.* 2023, *in press*. [CrossRef]
16. Salem, E.A.; Farid Khalil, M.; Sanhoury, A.S. Optimization of Insulation Thickness and Emissions Rate Reduction during Pipeline Carrying Hot Oil. *Alex. Eng. J.* **2021**, *60*, 3429–3443. [CrossRef]
17. Abujab, M.; Abusafa, A. Optimal Insulation's Thickness of Pipes in Variable Refrigerant Flow (VRF) System—An-Najah Child Institute as a Case Study. *Energy Rep.* **2022**, *8*, 321–330. [CrossRef]
18. Ucar, A. A Thermo-Economic Approach for Determination of Optimum Thickness of Thermal Insulation Applied to Piping Systems. *J. Renew. Sustain. Energy* **2018**, *10*, 035102. [CrossRef]
19. Keçebaş, A.; Ali Alkan, M.; Bayhan, M. Thermo-Economic Analysis of Pipe Insulation for District Heating Piping Systems. *Appl. Therm. Eng.* **2011**, *31*, 3929–3937. [CrossRef]
20. Zhukov, A.; Medvedev, A.; Poserenin, A.; Efimov, B. Ecological and Energy Efficiency of Insulating Systems. *E3S Web Conf.* **2019**, *135*, 03070. [CrossRef]
21. Zhang, T.; Li, A.; Hari, Q.; Li, X.; Rao, Y.; Tan, H.; Du, S.; Zhao, Q. Economic Thickness and Life Cycle Cost Analysis of Insulating Layer for the Urban District Steam Heating Pipe. *Case Stud. Therm. Eng.* **2022**, *34*, 102058. [CrossRef]
22. Wang, Y.; Tu, Z.; Yuan, L. Analysis of Thermal Energy Storage Optimization of Thermal Insulation Material and Thermal Insulation Structure of Steam Pipeline. *Therm. Sci.* **2020**, *24*, 3249–3257. [CrossRef]
23. Krasnova, N.P.; Gorshenin, A.S.; Rakhimova, J.I. Gas-Filled Thermal Insulation Use in Heat Supply. *IOP Conf. Ser. Earth Environ. Sci.* **2019**, *288*, 012099. [CrossRef]
24. Patel, M.; Mehta, B. Optimize Thermal Insulation. *Hydrocarb. Process.* **1993**, *72*, 51–55.
25. Zhang, L.; Zou, Y.; Yang, Y.; Chen, X.; Dai, Y.; Zhou, C.; Xu, H. Design and Optimization of Thermal Insulation Structure for High-Temperature Pipeline inside the Lower Tank Wall. *Ann. Nucl. Energy* **2023**, *192*, 109988. [CrossRef]
26. Sutheesh, P.M.; Chollackal, A. Thermal Performance of Multilayer Insulation: A Review. *IOP Conf. Ser. Mater. Sci. Eng.* **2018**, *396*, 012061. [CrossRef]
27. Dye, S.; Kopelove, A.; Mills, G.L. Wrapped Multilayer Insulation for Cryogenic Piping. *AIP Conf. Proc.* **2012**, *1434*, 1293–1298. [CrossRef]
28. Afroozeh, M.; Abdolmohammadi, H.R.; Nazari, M.E. Economic-Environmental Dispatch of Integrated Thermal-CHP-Heat Only System with Temperature Drop of the Heat Pipeline Using Mutant Gray Wolf Optimization Algorithm. *Electr. Power Syst. Res.* **2022**, *212*, 108227. [CrossRef]
29. Afra, M.; Peyghambarzadeh, S.M.; Shahbazi, K.; Tahmassebi, N. Thermo-Economic Optimization of Steam Injection Operation in Enhanced Oil Recovery (EOR) Using Nano-Thermal Insulation. *Energy* **2021**, *226*, 120409. [CrossRef]
30. Yang, J.; Lourenço, M.I.; Estefen, S.F. Thermal Insulation of Subsea Pipelines for Different Materials. *Int. J. Press. Vessel. Pip.* **2018**, *168*, 100–109. [CrossRef]
31. Kayfeci, M.; Yabanova, İ.; Keçebaş, A. The Use of Artificial Neural Network to Evaluate Insulation Thickness and Life Cycle Costs: Pipe Insulation Application. *Appl. Therm. Eng.* **2014**, *63*, 370–378. [CrossRef]
32. Xu, Y.; Zhang, Y.; Liu, X.; Ma, C.; Liu, L. Research on Thermal Insulation Performance of Composite Energy Storage Pipeline with Phase Change Materials. *J. Energy Storage* **2022**, *55*, 105711. [CrossRef]
33. Sahin, A.Z.; Kalyon, M. Maintaining Uniform Surface Temperature along Pipes by Insulation. *Energy* **2005**, *30*, 637–647. [CrossRef]
34. Zaki, G.M.; Al-Turki, A.M. Optimization of Multilayer Thermal Insulation for Pipelines. *Heat Transf. Eng.* **2000**, *21*, 63–70. [CrossRef]
35. Zhang, Z.; Zhou, D.; Lim, Y.M.; Fang, H.; Huo, R. Analytical Solutions for Multilayered Pipes with Temperature-Dependent Properties under Non-Uniform Pressure and Thermal Load. *Appl. Math. Model.* **2022**, *106*, 369–389. [CrossRef]
36. Kim, J.H.; Park, D.K.; Kim, T.J.; Seo, J.K. Thermal-Structural Characteristics of Multilayer Vacuum-Insulated Pipe for the Transfer of Cryogenic Liquid Hydrogen. *Metals* **2022**, *12*, 549. [CrossRef]

37. Zeng, Q.; Jiang, H.; Liu, Q.; Li, G. A Method for Measuring Interlayer Vacuum Degree of the Liquified Natural Gas Vacuum Multilayer Insulation Pipe by Temperatures. *Instrum. Exp. Technol.* **2022**, *65*, 818–825. [CrossRef]
38. Vakulenko, D.; Mileikovskyi, V.; Tkachenko, T.; Ujma, A.; Konovaliuk, V. Analysis of Critical Radius of Insulation Horizontal Pipes. *Eng. Rural. Dev.* **2023**, *24*, 902–907. [CrossRef]

Disclaimer/Publisher's Note: The statements, opinions and data contained in all publications are solely those of the individual author(s) and contributor(s) and not of MDPI and/or the editor(s). MDPI and/or the editor(s) disclaim responsibility for any injury to people or property resulting from any ideas, methods, instructions or products referred to in the content.